Anal. Chem. **2007,** *79,* 4729−4735

Photonic Crystal Surface Waves for Optical Biosensors

Valery N. Konopsky* and Elena V. Alieva

Institute of Spectroscopy, Russian Academy of Sciences, Troitsk, Moscow region, 142190, Russia

We present a new optical biosensor technique based on registration of dual optical s-polarized modes on a photonic crystal surface. The simultaneous registration of two optical surface waves with different evanescent depths from the same surface spot permits the segregation of the volume and the surface contributions from an analyte, while the absence of metal damping permits an increase in the propagation length of the optical surface waves and the sensitivity of the biosensor. Our technique was tested with the binding of biotin molecules to a streptavidin monolayer that has been detected with signal/noise ratio of ∼15 at 1-s signal accumulation time. The detection limit is ∼20 fg of the analyte on the probed spot of the surface.

Optical biosensors have played a key role in the selective recognition of target biomolecules and in biomolecular interaction analysis, providing kinetics data of biological binding events in real time without labeling. Advantages of the label-free concept are the elimination of undue detrimental effects from labels that may interfere with fundamental interaction and the absence of a time-consuming pretreatment.[1] Disadvantages of all label-free techniques, including the most mature one, surface plasmon resonance (SPR) technique,[2] are a deficient sensitivity to a specific signal and undesirable susceptibilities to nonspecific signals, e.g., to the volume effect of refraction index variations. Our goal was to overcome these variations caused by temperature fluctuations and drifts that are a problem for many state-of-the-art optical biosensors.

Registration of optical waves propagating along the surface under investigation is the most used method in the label-free optical biosensors.[3] In the SPR technique, these waves are surface plasmon polaritons[4] propagating along a gold or silver surface, while in the resonant mirror technique,[5] the waves are waveguide modes excited in a high refractive index dielectric layer via the frustrated total internal reflection (TIR) from a low refractive index spacer. In both cases, an evanescent field of the optical wave (with penetration depth in water ∼100 nm) is sensitive not only to biomolecular interactions at the surface but also to changes in the volume refraction index (RI) of the liquid due to variations of the liquid temperature, composition, and so on. For example, a water temperature change of 0.1 °C gives a water RI change of $\sim 10^{-5}$.

Therefore, a need exists for a biosensor technique that would be able to segregate the volume and the surface contributions from an analyte in detected signals. To obtain these two parameters, one needs to detect at least two optical waves with different characteristics (e.g., with different penetration depths) simultaneously. In the work,[6] we exploited a bulk optical wave, propagating above the sensing surface as a reference of the volume RI fluctuations. The weakness of this method is the impossibility of decreasing the flow cell height (and therefore the flow cell volume) because of using the bulk optical wave.

Slavík et al.[7] have tried to use the excitation of long-range and short-range plasmons at the same surface spot by polychromatic light at fixed incident angle (so-called wavelength interrogation—the spectrum of the reflected light is examined) to separate bulk from surface effects. Authors claimed a noise-limited resolution of their method is 11 times worse than the one of an ordinary SPR method with wavelength interrogation (which itself is less sensitive than an angular interrogation method). The reason is a very small propagation length of the short-range plasmons. Moreover, the excitation of both modes at the same incident angle means that these modes differ little in their penetration depths, because the penetration depth difference here is originated from a wavelength difference of these modes only (see eq 1 below).

In a dual-waveguide interferometric technique[8] the measurement of propagation constants of two modes with s- and p-polarizations is used to seek an adsorption layer thickness and its RI. It is worth noting here that the exploitation of the modes with the orthogonal polarizations may be stated as a weakness of the method, because of an implicit assumption that the adlayer is an isotropic substance, while the adlayer is almost always anisotropic (and birefringent to some extent) due to its binding to the surface.

Here we present a technique based on the simultaneous registration of two s-polarized optical surface waves on a one-dimensional photonic crystal surface. Photonic crystals (PCs) are materials that possess a periodic modulation of their refraction index on the scale of the wavelength of light.[9] Such materials can

* To whom correspondence should be addressed. E-mail: konopsky@isan.troitsk.ru.

(1) Cooper, M. A. *Anal. Bioanal. Chem.* **2003**, *377*, 834−842.
(2) Homola, J.; Yee, S. S.; Gauglitz, G. *Sens. Actuators, B* **1999**, *54*, 3−15.
(3) Robinson, G. *Sens. Actuators, B* **1995**, *29*, 31−36.
(4) Raether, H. *Surface Plasmons*; Springer: Berlin, 1988.
(5) Cush, R.; Cronin, J.; Stewart, W.; Maule, C.; Molloy, J.; Goddard, N. *Biosens. Bioelectron.* **1993**, *8*, 347−353.
(6) Alieva, E. V.; Konopsky, V. N. *Sens. Actuators, B* **2004**, *99*, 90−97.
(7) Slavík, R.; Homola, J.; Vaisocherová, H. *Meas. Sci. Technol.* **2006**, *17*, 932−938.
(8) Cross, G.; Reeves, A.; Brand, S.; Swann, M.; Peel, L.; Freeman, N.; Lu, J. *J. Phys. D: Appl. Phys.* **2004**, *37*, 74−80.
(9) Yablonovitch, E. *J. Opt. Soc. Am. B* **1993**, *10*, 283−295.

10.1021/ac070275y CCC: $37.00
Published on Web 05/12/2007

exhibit photonic band gaps that are very much like the electronic band gaps for electron waves traveling in the periodic potential of the crystal. In both cases, frequency intervals exist where the wave propagation is forbidden. This analogy may be extended[10] to include surface levels, which can exist in band gaps of electronic crystals. In PCs, they correspond to optical surface waves with dispersion curves located inside the photonic band gap.

The one-dimensional photonic crystal (1D PC) is a simple periodic multilayer stack. Optical surface modes in 1D PCs were studied in the 1970s, both theoretically[11] and experimentally.[12] Twenty years later, the excitation of optical surface waves in a Kretschmann-like configuration was demonstrated.[13] Despite several theoretical proposals[13,14] that suggested that the photonic crystal surface waves (PC SWs) have the potential to be superior alternatives in sensor applications to surface plasmons (due to low damping of PC SWs), there are no experimental demonstrations of such applications to date. In our opinion, the reason is the above-mentioned point that the limiting factor for the SPR technique is not the instrumental sensitivity but the temperature fluctuations and drifts. From this point of view, the increase of a propagation length of surface waves itself is ineffective without a concurrent compensation of the fluctuations of the liquid.

We show that in addition to the low loss propagation (which is not unique among other all-dielectric biosensors), the presented technique based on dual optical surface waves in 1D PCs has some additional advantages over all the above-mentioned biosensor techniques. Unique tunable properties of 1D PCs permit the design of a 1D PC structure that can support two long-range surface modes at the same wavelength (this is impossible in the SPR technique), with one mode exited very close to the angle of TIR from the water (this is unfeasible in any other waveguide techniques). The mode, in which the exited angle is infinitesimally close to the angle of TIR from the external medium, has a very large penetration depth in this medium (e.g., water) and may be used as a reference of bulk RI fluctuations. Indeed, the weak localization of this mode reduces its sensitivity to overlayers and increases its sensitivity to changes in the bulk RI. Simultaneous detection of two modes, with one of them being more sensitive to changes of the RI of the liquid then the other, permits us to derive both the RI of the liquid, $n_e = n_e(\rho_1, \rho_2)$, and the adlayer thickness, $d_a = d_a(\rho_1, \rho_2)$, as functions of the detected angular parameters ρ_1 and ρ_2 of two PC SWs.

EXPERIMENTAL SECTION

Photonic Crystal Structure. The following 1D PC structure was used in experiments: substrate/$(LH)^3L'$/water, where L is a SiO_2 layer with thickness $d_1 = 154.0$ nm, H is a Ta_2O_5 layer with $d_2 = 89.4$ nm, and L' is a SiO_2 layer with $d_3 = 638.5$ nm. The SiO_2/Ta_2O_5 7-layer structure (started and finished by SiO_2 layers) was deposited by ion sputtering. The prism and substrate were made from BK-7 glass. The RIs of the substrate, SiO_2, Ta_2O_5, and water at $\lambda = 532$ nm, were $n_0 = 1.52$, $n_1 = n_3 = 1.49$, $n_2 = 2.12$, and $n_e = 1.335$, correspondingly. The RIs at other wavelengths were derived using dispersion data presented by Palik.[15]

Absolute Angle Measurements. The excitation angles of the optical surface waves, indicated as black diamonds in Figure 1, were experimentally measured with an angular accuracy of ±1′ by parallel laser beam at two wavelengths: $\lambda = 532$ nm (second harmonic of Nd:YAG laser) and $\lambda = 442$ nm (He−Cd laser).

Materials. All biochemicals (except streptavidin) were purchased from Sigma-Aldrich and were used immediately after preparation. A dialkoxyaminosilane 3-(2-aminoethylamino)propyldimethoxymethylsilane (molecular weight 206.36) was used to convert an OH-terminated SiO_2 surface to an NH_2-terminated one.[16] Biotin-XX, sulfosuccinimidyl ester sodium salt (or Sulfo-NHS-LC−LC-Biotin; molecular weight, 669.74; mass added to target, 452.6) was used for the biotinylation of the amino-terminated surface. The streptavidin from Amersham (molecular weight $M_{str} \sim 60\,000$) was deposited on the biotinylated surface. The free biotin (vitamin H; molecular weight $M_b = 244.31$) was used as a test for detection of small-molecule binding with a streptavidin monolayer. All experiments were done in the phosphate-buffered saline (PBS; pH 7.2) except absolute angle measurements of PC SW excitation, which were done in pure water.

Sample Preparation. Samples (i.e., their top silicon oxide layers with thickness 638.5 nm) were cleaned as follows: first, they were sonicated in ethanol and acetone for 5 min each and then immersed into a piranha solution (H_2SO_4 (95%)/H_2O_2 (30%) = 3:1) for 15 min (caution, piranha solution reacts violently with organic solvents). The glass slides were then exposed to UV−ozone (185 and 254 nm) for 45 min and finally thoroughly rinsed with DI water. The precleaned glass slides (with expected OH bonds on the SiO_2 surface) were immersed in 1% aminosilane solution in 95% acetone/water for 5 min. The slides were then rinsed with acetone and baked for 30 min at 120 °C. Then the sample was mounted in the flow cell, and further sample treatment was made in situ. For the biotinylation of the NH_2-terminated surface of the slides, Sulfo-NHS-LC−LC-Biotin (2 mg/mL in PBS) was flowed over the flow cell for several minutes, then the fluid flow was stopped for several hours or even overnight, and the biotinylation of the surface was monitored in real time. Then the flow cell system was thoroughly rinsed by PBS.

Liquid Handling. The flow cell consists of a glass slide with two holes in which two glass tubes are fitted, serving as inlet and outlet, respectively. The height of the cell is determined by a thickness of a Teflon film, which serves as a sealing gasket and as a spacer between the sample and the glass slide. We have used the Teflon films with thicknesses 35 or 100 μm. The flow cell volume was 3.5 or 10 μL, correspondingly. The dead volume of the flow cell system was ~25 μL. Gravity flows of streptavidin or biotin solutions and pure PBS buffer were used with volumetric flow rate up to 1 mL/min.

Angular Resonance Curve Measurements. The angular resonance curves in Figure 2b were measured by focusing both parts of the splitted laser beam (with diameter $D \simeq 3$ mm) in the same spot on the structure surface with the objective of a focal length of $f = 60$ mm and detecting the intensity distribution of

(10) Kossel, D. *J. Opt. Soc. Am.* **1966**, *56*, 1434−1434.
(11) Yeh, P.; Yariv, A.; Hong, C.-S. *J. Opt. Soc. Am.* **1977**, *67*, 423−438.
(12) Yeh, P.; Yariv, A.; Cho, A. Y. *Appl. Phys. Lett.* **1978**, *32*, 104−105.
(13) Robertson, W. M.; May, M. S. *Appl. Phys. Lett.* **1999**, *74*, 1800−1802.
(14) Villa, F.; Regalado, L.; Ramos-Mendieta, F.; Gaspar-Armenta, J.; Lopez-Rios, T. *Opt. Lett.* **2002**, *27*, 646−648.
(15) Palik, E. D. *Handbook of Optical Constants of Solids*; Academic: London, 1985.
(16) Li, J.; Wang, H.; Zhao, Y.; Cheng, L.; He, N.; Lu, Z. *Sensors* **2001**, *1*, 53−59.

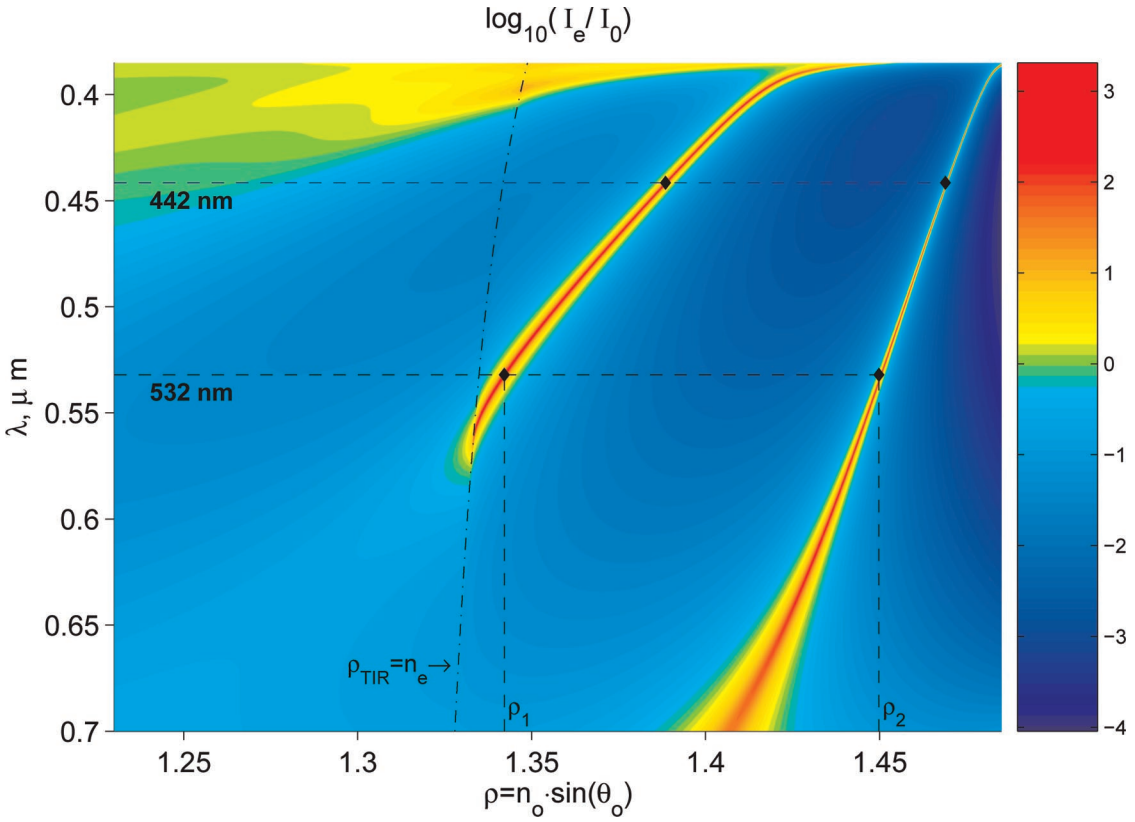

Figure 1. Calculated dispersion of the 7-layer PC structure in water and measured experimental points (black diamonds) at $\lambda = 532$ nm and $\lambda = 442$ nm laser wavelengths. The two optical surface modes are clearly seen as red curves (with an enhancement ~1000) inside the band gap (with an enhancement much less than 1).

reflected light with a 512-pixel Hamamatsu photodiode array placed 385 mm|442 mm ($\rho_1|\rho_2$) apart from the structure as shown in Figure 2a. The dynamic range of the angular measurements is $\pm D/(2f) = \pm 0.025$ rad that corresponds to the external media RI change $\Delta n \simeq \pm 0.035$ or to the adlayer thickness deposition $\Delta d \simeq \pm 120$ nm.

Data Handling. Data acquisition from the diode array, data processing, and presentation were done with homemade software we wrote on a personal computer running under Windows.

RESULTS AND DISCUSSION

We prepared the test photonic crystal structure and measured absolute angles of the PC SW excitation at two wavelengths: $\lambda = 532$ nm and $\lambda = 442$ nm. In Figure 1, a calculated dispersion of our 1D PC structure in water is presented as the logarithm of optical field enhancement (i.e., as $\lg[(E_e E_e^*)/(E_0 E_0^*)]$) in the external medium near the structure. Good correspondence is seen between experimental points (black diamonds) and the calculated dispersion curves of the surface modes. The dispersion is presented in coordinate $\lambda(\rho)$, where λ is an optical wavelength and ρ is a numerical aperture $\rho = n_0 \sin(\theta_0)$. The numerical aperture ρ may be used as an angle variable instead of angles θ_j in different layers. This is a unified angle variable for all layers since, according to Snell's law, $\rho = n_0 \sin(\theta_0) = n_j \sin(\theta_j)$, for any layer j. The angular parameter ρ, at which the excitation of a surface mode occurs, is equal to an effective RI of the mode. Therefore, the two red curves in Figure 1 present the dispersion of the two optical surface modes (i.e., the dependence of theirs effective RI from the wavelength).

From Figure 1, one can see that it is possible to excite one of the PC SWs in proximity to the TIR angle from the water by appropriately choosing the laser wavelength or by appropriately choosing the PC structure. The penetration length of the evanescent wave intensity (i.e., $E_e E_e^*$) in the external medium, which is

$$l_e = \frac{\lambda}{4\pi\sqrt{\rho_1^2 - \rho_{TIR}^2}} \quad (1)$$

may be very large for this mode if the difference $(\rho_1 - \rho_{TIR}) = (\rho_1 - n_e)$ is small. This is a unique property of PC SWs, because in any standard waveguide techniques,[5,8] the numeric aperture or (in other words) the effective RI of the waveguide mode ρ_{mode} is always more then a RI of the low refractive index spacer n_{spacer}. Therefore, the difference $(\rho_{mode} - \rho_{TIR}) \geq (n_{spacer} - n_e)$ cannot be made small in the standard waveguides, taking into account the RI of the water ($n_e \simeq 1.33$) and the RI of the spacer (usually made from SiO_2, $n_{spacer} \simeq 1.49$).

Another unique property of PC SWs is the possibility to excite them in the structure, where the final dielectric layer (the silicon oxide layer in our case) may have a low RI, while the standard waveguide has a high RI layer on a low RI spacer. This simplifies the procedures of biochemical modification of the external surface, which is now the standard SiO_2 surface.

In Figure 2, the biosensor setup scheme and a typical raw experimental signal from the setup are shown. The Hamamatsu photodiode array was used to record the experimental signals—angles of two PC SWs (ρ_1 and ρ_2) simultaneously. The interference

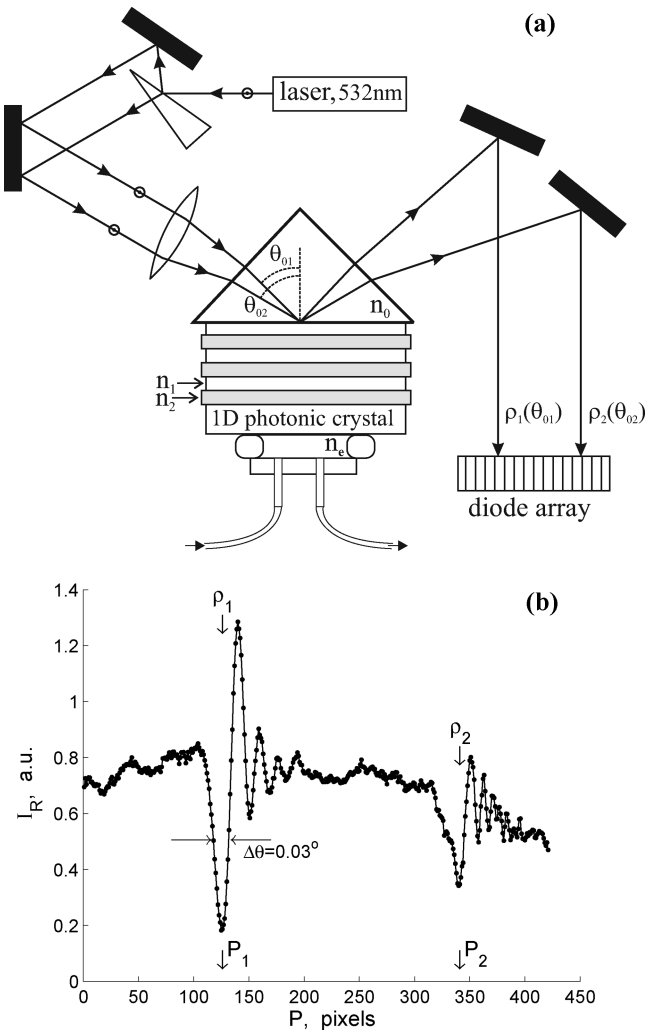

Figure 2. Biosensor scheme (a) and a typical raw experimental signal from the diode array (b).

near resonance curves is the distinguishing feature of long-range PC SW propagation. We observed similar interference in our recent work,[17] dealing with long-range surface plasmon polaritons propagation. The appearance of such interference means that the propagation distance of the PC SW becomes much more than the waist of an incident Gaussian beam at the surface (this also may be easily seen on the sample surface by the naked eye). In ref 17, the origin of this interference is described in more detail. Note that the resonance peaks in Figure 2b are very sharp (due to the long-range PC SW propagation), and this allows measurement of the resonance peaks position change with high precision.

The changes of the resonance peak positions P_1 and P_2 may be converted to changes of the resonance angles $\Delta\rho_1$ and $\Delta\rho_2$. To derive the changes of the RI of the liquid and the adlayer thickness from the changes of the resonance angles of two PC SWs, we use two independent methods, which give similar results if the changes are small.

The first method is based on an analysis of influence of the adlayer deposition and the bulk RI changes on the dispersion relation of the two optical surface modes. This method is in need of absolute values of the resonance angular parameters ρ_1 and ρ_2 and generates the absolute values of the RI of the external medium, $n_e = n_e(\rho_1, \rho_2)$, and the adlayer thickness, $d_a = d_a(\rho_1, \rho_2)$. The equations derived in the first method are cumbersome and not presented here.

The second method is a pure linear method, based on the Taylor expansion. It is in need of relative changes $\Delta\rho_1$, $\Delta\rho_2$ and generates the relative changes of the RI of the liquid, $\Delta n = \Delta n(\Delta\rho_1, \Delta\rho_2)$, and relative changes of the adlayer thickness, $\Delta d = \Delta d(\Delta\rho_1, \Delta\rho_2)$. In the second method, we take Taylor expansion of both resonance angle changes in terms of Δn and Δd:

$$\Delta\rho_1 = \Delta_n\rho_1 + \Delta_d\rho_1 = \frac{\partial\rho_1}{\partial n}\Delta n + \frac{\partial\rho_1}{\partial d}\Delta d \qquad (2a)$$

$$\Delta\rho_2 = \Delta_n\rho_2 + \Delta_d\rho_2 = \frac{\partial\rho_2}{\partial n}\Delta n + \frac{\partial\rho_2}{\partial d}\Delta d \qquad (2b)$$

From these equations, we obtain the desired values as functions of measured $\Delta\rho_1$ and $\Delta\rho_2$:

$$\Delta_n\rho_1 = \frac{\partial\rho_1}{\partial n}\Delta n = \frac{\Delta\rho_1 - \Delta\rho_2/K_d}{1 - K_n/K_d} \qquad (3a)$$

$$\Delta_d\rho_2 = \frac{\partial\rho_2}{\partial d}\Delta d = \frac{\Delta\rho_2 - K_n\Delta\rho_1}{1 - K_n/K_d} \qquad (3b)$$

where K_d and K_n are the ratio of the corresponding partial derivatives:

$$K_d = \frac{\partial\rho_2}{\partial d}\Big/\frac{\partial\rho_1}{\partial d} \qquad (4a)$$

$$K_n = \frac{\partial\rho_2}{\partial n}\Big/\frac{\partial\rho_1}{\partial n} \qquad (4b)$$

To obtain a dimensionless value proportional to Δn in one channel, and a dimensionless value proportional to Δd in another channel, we need only K_d and K_n coefficients (see the right-hand side of eqs 3a and 3b). If we want to have Δn in RI units and Δd in length units, we also need $\partial\rho_1/\partial n$ and $\partial\rho_2/\partial d$ correspondingly. All these coefficients may be obtained, for example, from a theoretical simulation of the real 1D PC structure. For the presented structure, these coefficients are, $K_d = 0.415$; $K_n = 0.1$; $\partial\rho_1/\partial n = 0.5(1/\text{RI})$ and $\partial\rho_2/\partial d = 0.06(1/\mu\text{m})$ (assuming that the adlayer RI is $n_a = 1.43$).

To verify the sensitivity of the biosensor and to compare it with existing label-free methods, we present the unsmoothed experimental data of free biotin binding on the streptavidin monolayer. Initially (Figure 3a), we present the buildup of the streptavidin monolayer on the biotinylated surface. Streptavidin (diluted in PBS to a concentration of $c_{str} = 16\ \mu\text{g/mL}$) was run through the flow cell with volumetric flow rate $v_{str} = 0.4$ mL/min. Then the flow cell was rinsed by PBS. In Figure 3a, one can see that the adlayer thickness increases on 6.2 nm during streptavidin binding to biotinylated surface. All presented in Figure 3 data are obtained by the first method, based on the dispersion relation analysis.

(17) Konopsky, V. N.; Alieva, E. V. *Phys. Rev. Lett.* **2006**, *97*, 253904.

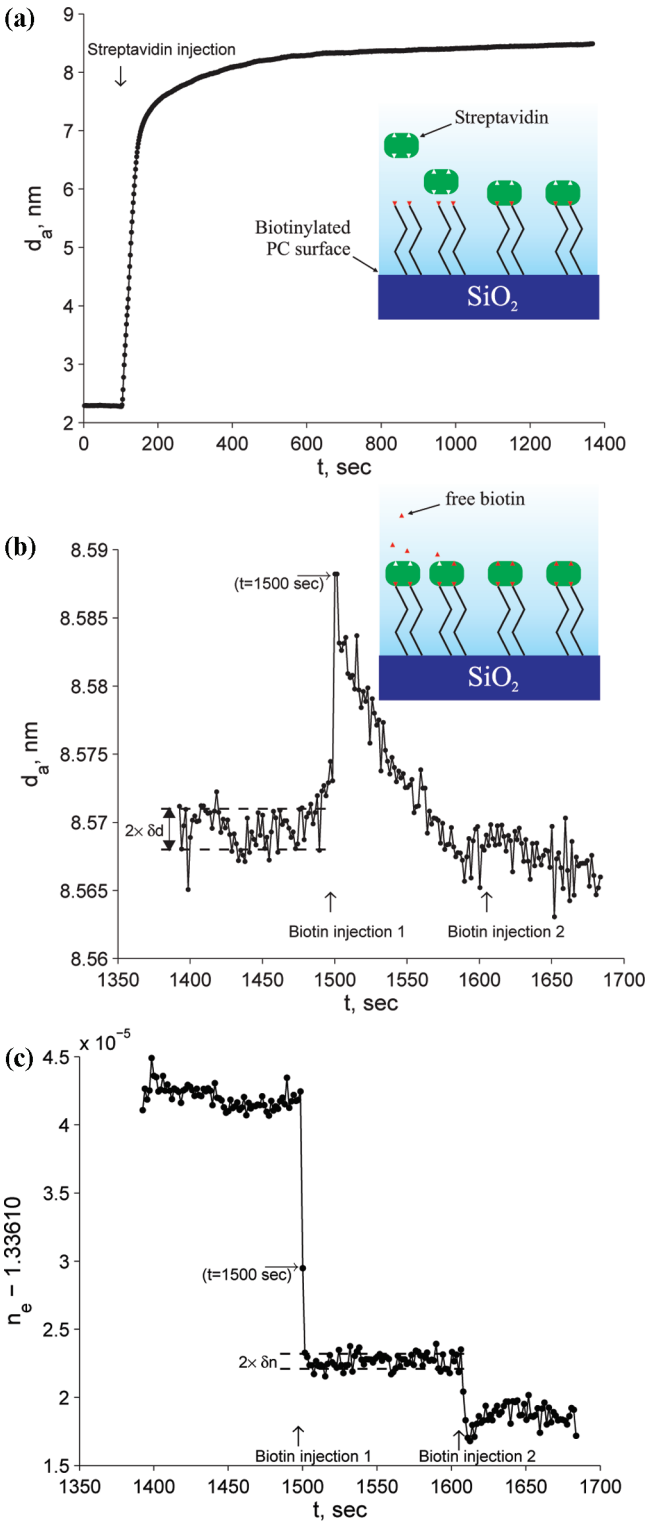

Figure 3. Immobilization of streptavidin on a biotinylated surface (a) and free biotin binding to the streptavidin monolayer: changes of the layer thickness (b) and RI of the buffer (c). The measurement time is 1 s per point (no posterior data averaging and smoothing). In color insets, the corresponding processes are illustrated.

Figure 3b presents the change of d_a during free biotin binding to the streptavidin monolayer, while Figure 3c shows RI changes of the analyte during these biotin solution injections. Biotin (in a concentration of $c_b = 3$ μg/mL) was injected into PBS running through the flow cell with volumetric flow rate $v_b = 0.6$ mL/min. Figure 3b shows that the streptavidin monolayer at first increases its thickness but then contracts to a value slightly less than the initial one. At the same time, Figure 3c shows that the external medium RI is not changed until the second biotin injection (from 1501 to 1600 s, $n_e \simeq$ const). So, in Figure 3b, in this time period, we observe the act of streptavidin conformation during (or after) biotin molecule penetration into binding pockets of streptavidin molecules. The second biotin injection did not result in the same streptavidin conformation, because most streptavidin subunits are already occupied by biotin molecules.

Before proceeding further, it is worth estimating the characteristic times of the processes under study. The upper limit of a mass transport kinetics (by a combination of convection and diffusion) in our flow cell may be estimated by the so-called Smoluchowski–Levich approximation[18,19]

$$j_0 = ck_m = c\left(\frac{D}{h}\right)^{2/3}\left(\frac{v}{wx}\right)^{1/3} \quad (5)$$

where j_0 (molecules/(s cm^2)) is deposition rate of molecules (with concentration c (molecules/cm^3) and with a diffusion coefficient D (cm^2/s)) on the sensing surface, which is considered as an ideal collector. Parameters of our flow cell are as follows: $h = 0.01$ cm – height, $w = 1$ cm – width, $x = 0.4$ cm – distance from flow chamber entrance and v is the volumetric flow rate (cm^3/s). The diffusion coefficient of a streptavidin molecule may be estimated by the Stokes–Einstein equation:

$$D_{str} = \frac{kT}{6\pi\eta R_{str}} \simeq 7 \times 10^{-7}\ \text{cm}^2/\text{s} \quad (6)$$

where we take the streptavidin molecule diameter $2R_{str} = 6.2$ nm (see above), water viscosity $\eta \simeq 10^{-2}$ g/(cm s), and Boltzmann constant $k = 1.38 \times 10^{-16}$ g cm^2/(s^2 grad). The diffusion coefficient of a biotin molecule may be estimated by assuming that its effective radius is $R_b = R_{str}(M_b/M_{str})^{1/3}$. In this case, $D_b = 4.3 \times 10^{-6}$ cm^2/s.

Now we can estimate the time it takes the combination of convection and diffusion to supply a required number of molecules N for the monolayer cover of a probed spot on the surface. It is

$$t = \frac{N}{j_0 S} \quad (7)$$

where S is the area of a probed spot on the surface. The probed spot on the surface is determined by the size of the laser beam focus $\omega_0 \simeq 50$ μm and by the propagation length of the optical surface waves $L \simeq 2$ mm. Therefore, an area of the probed spot is $S = \omega_0 L \simeq 0.1$ mm^2. Assuming that one streptavidin molecule occupies a square 10 × 10 nm^2 (i.e., ~10^{10} molecules/mm^2), we deduce that $N^{str} \simeq 10^9$ molecules were detected on our probed spot during the deposition presented in Figure 3a. Using (7), (5), and (6), we obtain the characteristic time of the mass transport of 10^9 streptavidin molecules to the probed spot of the surface, $t_{str} \simeq 14$ s, that corresponds well to the time of the linear increase in Figure 3a. From the same equations, we receive the next

(18) Elimelech, M. *Sep. Technol.* **1994**, *4*, 186–212.
(19) Myszka, D. G.; He, X.; Dembo, M.; Morton, T. A.; Goldstein, B. *Biophys. J.* **1998**, *75*, 583–594.

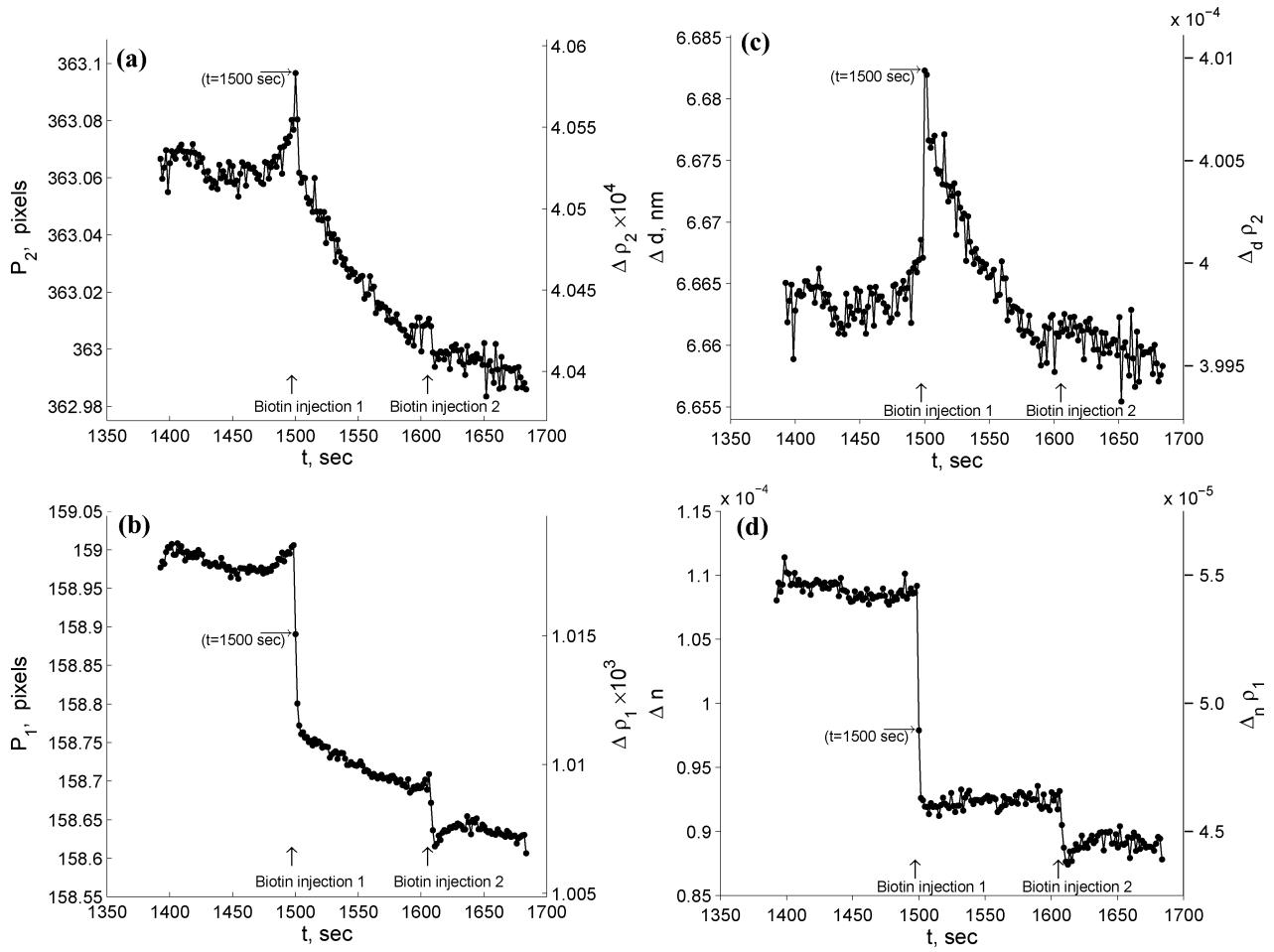

Figure 4. Initial data from the biosensor and theirs treatment by the linear method. (a) Movement of the second resonance mode in terms of pixels (left axis P_2) and in terms of angle changes (right axis $\Delta\rho_2$). (b) Movement of the first resonance mode (which is more sensitive to the bulk RI) in terms of pixels (left axis P_1) and in terms of angle changes (right axis $\Delta\rho_1$). (c) Calculated changes of the adlayer thickness in terms of $\Delta_d\rho_2$ (right axis) and in nanometers (left axis). (d) Calculated changes of the bulk RI in terms of $\Delta_n\rho_1$ (right axis) and in RI units (left axis).

characteristic time of the mass transport of $N^b = 2N^{str} \simeq 2 \times 10^9$ biotin molecules to the probed spot of the surface, $t_b \simeq 0.16$ s, i.e., less than the time of the single measurement (1 s). The biotin−streptavidin couple has extremely high binding affinity $K_A = k_{on}/k_{off} \sim 10^{13}$ (1/M), and therefore, the characteristic time of biotin−streptavidin binding estimated through its association constant $k_{on} \sim 7.5 \times 10^7$ (1/(M s))[20] is in the millisecond range (at the concentration c_b we used). However, the biotin−streptavidin association involved several transient intermediate steps, and the simple framework based on the single association constant appears insufficient for detailed description of this binding. The transient intermediate steps include desolvation of five bound water molecules in each biotin binding site. Then a flexible loop in streptavidin becomes immobilized after biotin binding in a biotin binding pocket and closes the biotin binding pocket (and, hence, shields a biotin molecule from competition with solvent).[21] The decrease of the streptavidin thickness in Figure 3b at 1501−1600 s may be this streptavidin postbinding conformational change needed for a stable interaction.

It may appear that the sharp thickness increase in Figure 3b (at 1499 s) is a data evaluation artifact due to sharp change of the bulk RI, because the kinetics of the increase looks very similar to the that of the decrease of the refractive index in Figure 3c. To be sure that it is not the case and that the adlayer thickness really increases after biotin injection, we present the initial data of resonance peak changes (Figure 4a and Figure 4b) and the treatment of the data (Figure 4c and Figure 4d) by our second method (i.e., by eqs 3a and 3b). From Figure 4a, one can see that the second resonance angle ρ_2 increases its value (at 1499−1500 s) after biotin solution injection, reaches its maximum at 1500 s and only then decreases, while the first resonance angle ρ_1 (which is more sensitive to the bulk RI) is sharply decreasing at 1499−1500 s (Figure 4b). Considering eq (2b) and keeping in mind that all partial derivatives in this equation are positive ($\partial\rho_2/\partial d$, $\partial\rho_2/\partial n > 0$) one can deduce that the increase of ρ_2 at 1499−1500 s may be the result of either the adlayer thickness increase or a bulk RI increase. But to exclude the latter interpretation, we have decreased the RI of the biotin solution in respect to RI of the PBS by adding 20 μL of the pure water in 1 mL of PBS with biotin (before the biotin solution injection). Since $n_{PBS} - n_{H_2O} \simeq 0.0012$, the change of the RI of the biotin solution (due to water injection) in respect of the RI of PBS is $\Delta n \simeq -2 \times 10^{-5}$, while the biotin itself in such small concentration practically does not change the RI of the PBS ($\Delta n_{biotin} < 10^{-7}$). This procedure was needed to be sure that the injection of the biotin solution will cause

(20) Hyre, D. E.; Trong, I. L.; Merritt, E. A.; Eccleston, J. F.; Green, N. M.; Stenkamp, R. E.; Stayton, P. S. *Protein Sci.* **2006**, *15*, 459−467.
(21) Freitag, S.; Trong, I. L.; Klumb, L.; Stayton, P. S.; Stenkamp, R. E. *Protein Sci.* **1997**, *6*, 1157−1166.

the bulk RI to decrease only. Therefore, the increase of ρ_2 at 1499−1500 s may be the result of the adlayer thickness increase only. The exact value of the corresponding calculated adlayer thickness increase Δd (but not its sign) in Figure 4c depends on the exactness of the numerical values of the coefficients pointed after eq 4. But, inasmuch as the expected bulk RI change $\Delta n \simeq -2 \times 10^{-5}$ corresponds well to the results from Figures 3c and Figure 4d (calculated with the same coefficients), we expect that the calculated value of the adlayer thickness increase Δd is also reasonably accurate. From Figures 3b,c and Figures 4c,d, one can see that our first (dispersion analysis) and the second (linear) methods of the initial data treatment give the very similar results (though, certainly, do not coincide point to point).

In compliance with the work,[22] we suppose that the process of the biotin−streptavidin binding is a good candidate for comparison of the signal/noise ratio of different label-free techniques. We believe that for comparison of the signal/noise ratio it is also very important always to point out the time of the measurement and the fact of posterior data averaging, smoothing, or both (which increase the effective measurement time). In other words, the noise should be reduced to $1/\mathrm{Hz}^{1/2}$ value. In our experiments, the signal accumulation time was 1 s per point and no posterior data averaging or smoothing was done. The noise (i.e., standard deviation − std) of the thickness measurement was equal $\partial d = \mathrm{std}(d_a) \simeq 1.3\ \mathrm{pm/Hz}^{1/2}$. The noise of the measurement of the external medium RI was $\partial n = \mathrm{std}(n_e) \simeq 5 \times 10^{-7}/\mathrm{Hz}^{1/2}$. In Figure 3b, one can see that we detected the streptavidin conformation process during free biotin binding with a $(\mathrm{signal/noise})_b$ ratio of ∼15. The deposition of the streptavidin monolayer was detected with a $(\mathrm{signal/noise})_{str}$ ratio of ∼5000. Taking into account the $(\mathrm{signal/noise})_{str}$ ratio, we obtain a minimal quantity of streptavidin molecules that may be detected at the probed spot of our setup: $N^{str}_{min} = N^{str}/(\mathrm{signal/noise})_{str} \simeq 200\ 000$ streptavidin molecules. This corresponds to a mass detection limit $m^{str}_{min} = N^{str}_{min} M_{str}/N_A \simeq 2 \times 10^{-14}$ g = 20 fg of the analyte on the probed spot of the surface ($N_A \simeq 6 \times 10^{23}$ is Avogadro's number). For biotin molecules, we have a minimal detectable quantity equal to $N^{b}_{min} = 2N^{str}/(\mathrm{signal/noise})_b \simeq 1.3 \times 10^8$ biotin molecules or $m^{b}_{min} = N^{b}_{min} M_b/N_A \simeq 50$ fg of the analyte on our probed spot. Here we have assumed that in the process presented in Figure 3b each streptavidin molecule picks up two biotin molecules. If a streptavidin molecule picks up only one biotin molecule than this minimal detected mass is twice as small. We believe that the noise of the presented technique could be further decreased by improving the quality of the dielectric multilayer coating and by decreasing the laser noise.

(22) Zybin, A.; Grunwald, C.; Mirsky, V. M.; Kuhlmann, J.; Wolfbeis, O. S.; Niemax, K. *Anal. Chem.* **2005**, *77*, 2393−2399.

CONCLUSIONS

We have employed the two different optical modes on the photonic crystal surface for the optical sensing of biomolecular interactions. Unique properties of photonic crystals were used for the excitation of optical waves along the photonic crystal surface so that the evanescent field of one wave penetrates much deeper into the liquid volume. This wave is used as a reference for the RI of the liquid. The simultaneous registration of the two modes, reported here as a proof of principle, gives a possibility to derive both the RI of the liquid and the adlayer thickness. This permitted us to segregate the volume and the surface signals from the analyte, increase the sensitivity of biomolecule detection, and record the act of streptavidin conformation during binding of biotin molecules. Independent registration of the adlayer thickness and the temperature-dependent RI of the liquid may be potentially useful for design of a temperature-controlled flow cell, which may be considered as a biochemical reactor for evaluation of temperature dependency of reactions at the surface.

ACKNOWLEDGMENT

The authors thank S. Grachev for the kind donation of some biochemicals and for helpful advises about surface preparation. This work was partly supported by the European Network of Excellence, NMP3-CT-2005-515703-2.

Received for review February 9, 2007. Accepted April 13, 2007.

AC070275Y